

Enantioselective Ion-Pair Chromatography of Phenolic 2-Dipropylaminotetralin Derivatives on Achiral Stationary Phases: An Experimental and Theoretical Study of Chiral Discrimination

Anders Karlsson,^a Kristina Luthman,^{b,*} Curt Pettersson^{a,*} and Uli Hacksell^b

Departments of ^aAnalytical and ^bOrganic Pharmaceutical Chemistry, Uppsala Biomedical Centre, Box 574, Uppsala University, S-751 23 Uppsala, Sweden

Karlsson, A., Luthman, K., Pettersson, C. and Hacksell, U., 1993. Enantioselective Ion-Pair Chromatography of Phenolic 2-Dipropylaminotetralin Derivatives on Achiral Stationary Phases: An Experimental and Theoretical Study of Chiral Discrimination. – Acta Chem. Scand. 47: 469–481.

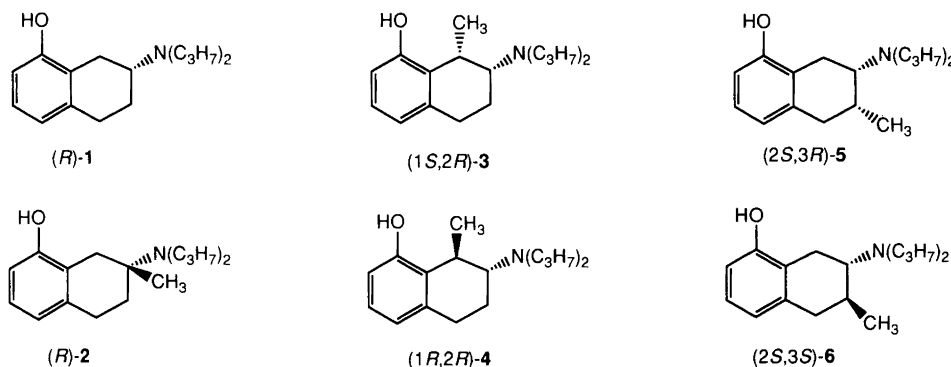
Separation of the enantiomers of six phenolic 2-dipropylaminotetralin derivatives by liquid ion-pair chromatography has been accomplished on an achiral stationary phase by the addition of a protected peptide derivative as a chiral selector to the mobile phase. The influence on the stereoselectivity and retention by the structure and concentration of the counterion and the properties of the stationary phase has been investigated. Maximal stereoselectivity was observed when benzyloxycarbonylglycyl-L-proline (L-ZGP) was used as a chiral selector on a porous graphitic carbon (Hypercarb) stationary phase. The separation factors (α) ranged from 1.0 to 3.46. When 8-hydroxy-2-dipropylaminotetralin was chromatographed in this system, the largest separation factors were observed at high counterion concentrations, indicating that the difference in adsorption constants between the diastereomeric complexes is responsible for the maximal stereoselective retention.

Complexes formed between L-ZGP and the various enantiomers were subjected to force-field (MMX) minimizations to determine the geometries and energies of energetically accessible complex conformers. The results of the calculations were used to determine various dynamic properties of the complexes, such as total and partial surface areas, dipole moments, binding energies and relative steric energies. A correlation ($r^2 = 0.80$) was observed between the separation factor α and the difference in dynamic unsaturated surface of the diastereomeric complexes.

Chromatographic separation of enantiomers may be achieved by indirect or direct techniques. The former, which are based on prederivatization of the enantiomers with chiral reagents, produce diastereomers that may be separated by achiral chromatography.¹ The direct techniques do not involve a prederivatization step using chiral reagents but utilize the ability of chiral stationary phases² or chiral additives³ in the mobile phase to separate enantiomers. The separation of enantiomers on chiral stationary phases is related to differences in stability and/or rate of formation of the diastereomeric complexes.

In separations of enantiomers by use of chiral additives the situation is more complex; the separation may be related to the stability of formation of complexes between the solute and the chiral selector. However, it may also be dictated by differences in the interaction between the diastereomeric complexes and the achiral stationary phase.

In the present investigation we have studied, by experimental and theoretical methods, factors of importance for the separation of the enantiomers of a set of phenolic 2-aminotetralins (**1–6**) by chiral ion-pair chromato-



graphy on achiral stationary phases. These separations were accomplished by the addition of a protected peptide derivative [e.g., *N*-benzyloxycarbonylglycyl-L-proline (L-ZGP)], as a chiral selector, to the eluent. A number of factors influencing the chromatographic results were studied including structure and concentration of the counterion, solid-phase and solute structure. In addition, for the complexes formed between L-ZGP and the enantiomers of 1–6, we calculated, by unrestricted molecular mechanics (MMX) minimizations, geometries and energies of complex conformations of accessible energy ($\Delta E_s \leq 3 \text{ kcal mol}^{-1}$). This information was used to determine dynamic measures⁴ of total and partial molecular surface areas, dipole moments and relative steric energies.

Methods

A. Experimental: materials. Porous graphitic carbon columns (Hypercarb) were obtained from Shandon. LiChrosorb DIOL, 2,4-dinitrophenol (*p.a.*) and dichloromethane (LiChrosolv) were purchased from Merck. Polygosil NH₂, Polygosil CN, Polygosil NO₂, Polygosil 7-OH and Nucleosil CN were bought from Macherey-Nagel. *N*-Benzyloxycarbonyl-L-proline (L-ZP) and *N*-benzyloxycarbonylglycylglycyl-L-proline (L-ZGGP) were obtained from Sigma. L-ZGP was obtained from Nova Biochem. *N*-Cyclopentylpropionyl-L-proline (L-CP) was synthesized⁵ at the Department of Analytical Pharmaceutical Chemistry. The syntheses of the enantiomerically pure as well as the racemic 2-aminotetralin derivatives used in this study have been reported previously.^{6–9} Triethylamine (Golden Label, >99%) was obtained from Fluka.

Chromatographic system. The chromatographic equipment consisted of a Constametric III pump, a Spectromonitor III UV-detector and a Rheodyne 7125 injector equipped with a 20 μl injection loop. The chromatographic system was kept at $21^\circ\text{C} \pm 0.1^\circ\text{C}$ with a waterbath HETO 02 PT 923 (Birkerød, Denmark).

Spectroscopy. ¹³C NMR spectroscopy was performed on a JEOL FX90Q spectrometer, whereas ¹H NMR spectra were run on a Varian VXR 400 spectrometer. CDCl₃ was used as the solvent and tetramethylsilane was used as an internal reference. IR spectra of CDCl₃ solutions were obtained on a Perkin-Elmer 298 IR spectrophotometer and UV absorption measurements on a Carl Zeiss M4 QIII UV spectrophotometer.

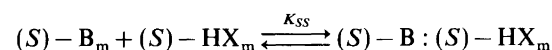
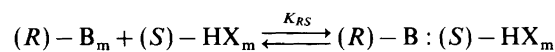
B. Molecular-mechanics calculations: general procedure. Energy-minimized geometries were obtained using the MMX force field which is included in the PCMODEL program (version PI 3.1).¹⁰ The calculations were performed without restrictions in the minimization process. The H-BND command was activated during each minimization in order to take into account potential

hydrogen bonds, and the default value of the relative permittivity (1.5) was used. The calculations were performed on IBM PS-2/70 A21 (25 MHz) or RM-486 (25 MHz) computers equipped with math-coprocessors. Computational times ranged from 20 min to 2 h per minimization.

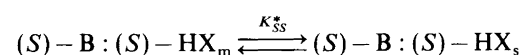
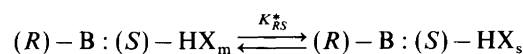
Evaluation of the MMX force field. It is of particular importance for the present study that the force field treats intermolecular interactions adequately. By analysis of the structures of the molecules docked in this study (L-ZGP and the 2-aminotetralins) we identified potentially important interactions: that is, electrostatic interactions, hydrogen bonding, attractive aromatic interactions and van der Waals interactions. Consequently, we analysed the ability of MMX to handle these types of intermolecular interactions. An investigation of model systems[†] indicated that MMX is able to treat these intermolecular interactions reasonably adequately, although the electrostatic component may be overestimated in the calculations.

Principles for enantioselectivity

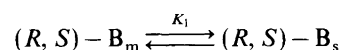
A. Basic equilibria. Enantioselectivity in ion-pair chromatography of 1–6 might be achieved if the ion-pair formation constants (K_{RS} and K_{SS}) differ in the mobile phase. The formation of diastereomeric complexes (ion-pairs) between the enantiomers of a chiral amine [(*R*)–B_m and (*S*)–B_m] and a chiral acid [(*S*)–HX_m] in the mobile phase are given by the equilibria below.



Separation of enantiomers might also be achieved if the adsorption to the stationary phase differs for the two diastereomeric complexes [(*R*)–B : (*S*)–HX_s and (*S*)–B : (*S*)–HX_s]. This is reflected in the constants K_{RS}^* and K_{SS}^* which are defined by the following equilibria.



One has to take into account that the 2-aminotetralins may be adsorbed to the achiral stationary phase as free amines [(*R*, *S*)–B_s] by an achiral mechanism according to the equilibrium below.



[†] The model systems used were: trimethylammonium acetate (electrostatic interactions), two benzene molecules (aromatic interactions) and two ethane molecules (van der Waals interactions), respectively.

B. An expression for ion-pair chromatographic separation of enantiomers. The capacity factor^{11,§} ($k'_{(R)-B}$) for the (*R*)-enantiomer is given by eqn. (1).

$$\begin{aligned} k'_{(R)-B} &= k'_{ac} + k'_{cR} \\ &= q \frac{C_{Bs}}{C_{Bm}} = q \frac{[(R)-B]_s}{[(R)-B]_m(1 + K_{RS}[(S)-HX]_m)} \\ &\quad + q \frac{[(R)-B : (S)-HX]_s}{[(R)-B : (S)-HX]_m \left(1 + \frac{1}{K_{RS}[(S)-HX]_m}\right)} \\ &= q \frac{K_1 + K_{RS}^* K_{RS} [(S)-HX]_m}{1 + K_{RS} [(S)-HX]_m} \end{aligned} \quad (1)$$

q is the phase volume ratio and C_{Bs} and C_{Bm} are the total concentrations of the amine in the stationary and the mobile phase, respectively. Eqn. (1) is based on the assumption that no side reactions occur in the mobile phase.

The separation factor is given schematically by eqn. (2).

$$\alpha_{S/R} = \frac{k'_S}{k'_R} = \frac{k'_{ac} + k'_{cS}}{k'_{ac} + k'_{cR}} \quad (2)$$

Insertion of the capacity factor [eqn. (1)] for the respective enantiomer gives eqn. (3).^{12,13}

$$\alpha_{S/R} = \frac{\left(K_1 + K_1 K_{RS} [(S)-HX]_m + K_{SS} K_{SS}^* [(S)-HX]_m + K_{SS} K_{RS} K_{SS}^* [(S)-HX]_m^2 \right)}{\left(K_1 + K_1 K_{SS} [(S)-HX]_m + K_{RS} K_{RS}^* [(S)-HX]_m + K_{RS} K_{SS} K_{RS}^* [(S)-HX]_m^2 \right)} \quad (3)$$

Thus, the chromatographic enantioselectivity may depend on the following factors: the concentration of the counterion and the value of the adsorption and/or ion-pair formation constants. At high counterion concentrations the separation factor becomes constant and depends, owing to the last term in eqn. (3), on differences in the adsorption properties of the diastereomeric ion-pairs, that is, $\alpha = K_{SS}^*/K_{RS}^*$. In the absence of counterion or at very low counterion concentrations, no enantioselectivity is obtained owing to the dominant first term in eqn. (3). Within a less extreme range of concentrations the separation factor may depend on the ion-pair formation constant and the adsorption constants as described by the two central terms in eqn. (3). It should be noted that the two processes giving chromatographic enantio-

selectivity, ion-pair formation and ion-pair adsorption, may counteract each other leading to a decrease in the separation factor.¹⁴ In order to predict the separation factor and the mechanism(s) that lead to enantioselectivity it is necessary to know the ion-pair formation and the adsorption constants.

Experimental results

A. Spectrophotometric determination of the ion-pair formation constant. The ion-pair formation constant (K_{SS}) of the (*S*)-enantiomer of **1** and L-ZGP (HX) dissolved in dichloromethane (500 ppm H₂O) was calculated using a spectrophotometric method presented previously.^{15,16¶} Three determinations of $\log K_{SS}$ are given in Table 1, the average being 4.0. The fraction of the chiral amine, which is present as a complex in dichloromethane ($[B : HX]_m/[B]_m$), could be calculated from the magnitude of the ion-pair formation constant and the counterion concentration. Using a mobile-phase concentration of L-ZGP of 10 mM, the ratio $[B : HX]_m/[B]_m$ is around 100, that is, the amine is present mainly as a complex in the mobile phase under the chromatographic conditions.

B. Spectroscopic studies of complexes: NMR experiments.

¹H NMR spectra of the two complexes formed in a CDCl₃ solution of equal amounts of L-ZGP and each of the enantiomers of **1** are notably similar, however, differences were observed in the region around the carbamate hydrogen ($\delta = 5.9$) and the glycyilmethylene moiety ($\delta = 4.0$) of L-ZGP. Both complexes show a predominant *cis*-arrangement around the glycyproline amide bond as indicated by the proline H _{α} -signals. The carbamate hydrogen appears as two well separated triplets in the spectrum of (*R*)-**1** : L-ZGP whereas the corresponding triplets overlap in the spectrum of (*S*)-**1** : L-ZGP (Fig. 1). These observations may be related to differences in carbamate conformations in the complexes and/or differences in hydrogen-bonding patterns. The glycyilmethylene region is different in the diastereomeric complexes indicating that the enantiomers of **1** interact with different conformers of L-ZGP (Fig. 1).

IR experiments. The diastereomeric complexes of L-ZGP and each of the enantiomers of **1** were also examined by IR spectroscopy. Dilute solutions of equal amounts of the complex components in CDCl₃ were examined. The spectral region around 3500 cm⁻¹, at which hydrogen bonding could be observed, was studied in detail. However, it was not possible to detect significant differences between the spectra of the diastereomeric complexes

[‡] Capacity factor (k') = $V_R - V_0/V_0$.

V_R = Retention volume of solute.

V_0 = Void volume.

[§] k'_{ac} = Achiral retention.

k'_{cR} = Chiral retention of the (*R*)-enantiomer.

[¶] The method uses competition between substrate acid (L-ZGP) and indicator acid (2,4-dinitrophenol) in ion-pairing to the phenolic aminotetralin. Large differences in the UV absorption spectra for free and complex-bound indicator acid were observed which made it possible selectively to measure the complex-bound indicator acid at 418 nm.

Table 1. Determination of the complex formation constant of L-ZGP and (S)-1 in dichloromethane (500 ppm H₂O).

[2,4-DNP]/mM ^a	[L-ZGP]/mM	[(S)-1]/mM	log K_{SS}
0.3235	0.2400	0.4808	4.1
0.3235	0.8018	0.4808	4.0
0.3235	0.8018	0.2404	3.9

^a [2,4-DNP] = 2,4-dinitrophenol (indicator acid).

which could reveal information on specific structural features of the complexes.

C. Chromatographic separations of enantiomers: the structure of the counterion. The effect of changing the structure of the chiral counterion on the enantioselective retention using a LiChrosorb DIOL phase was studied using the set of six enantiomeric pairs, 1–6. Four chiral counterions were used. The lowest separation factors ($\alpha < 1.05$) were obtained using L-CP and L-ZP as counterions (Table 2). The addition of one or two glycine residue(s) (L-ZGP and L-ZGGP, respectively) increased the enantioselectivity. Hence, the addition of an amide functionality improved the separation factors, probably as a result of additional possibilities for hydrogen bonding. The enantiomeric separation of regioisomers 1 and its 5-hydroxy analogue using L-ZGP and dichloromethane as the eluent is shown in Fig. 2.

The concentration of the counterion. The separation of the enantiomers increased with increasing concentration of the chiral selector in the mobile phase (Fig. 3). The chiral discrimination might be due to one, two or all

three of the terms giving enantioselectivity in eqn. (3). However, an increase of the chiral counterion concentration gives a final value of the separation factor that is equal to the ratio between the adsorption constants of the diastereomeric complexes ($\alpha = K_{SS}^*/K_{RS}^*$). In general it is difficult to predict the counterion concentration that gives the maximum separation factor, since the observed enantioselectivity may be the result of an additive or counteracting effect of mechanism A (differences in complex formation) and mechanism B (adsorption of the two diastereomeric complexes).

When racemic 1 was chromatographed on porous graphitic carbon the largest separation factors were observed at high counterion concentration (Fig. 3). This indicates that the difference in adsorption constants between the diastereomeric complexes is responsible for the maximal stereoselective retention.

The solid phase. The effect of six different silica phases and porous graphitic carbon (Hypercarb) on the stereoselective retention of 1 are given in Table 3. A solution of L-ZGP in dichloromethane was used as the mobile phase in experiments with Hypercarb as the stationary phase. However, on all the silica supports a competing amine (triethylamine, TEA)¹⁷ was added to the mobile phase in order to obtain reasonable retention times for the racemic solute and to obtain comparable chromatographic conditions. The various silica supports had different effects on the stereoselectivity ($\alpha_{K'S/K'R} = 1.10$ –1.24). The change in adsorption constants of the two diastereomeric complexes as well as the change in adsorption of the free amine gave rise to the variation in stereoselective retention. However, it was difficult to predict the degree of stereoselectivity

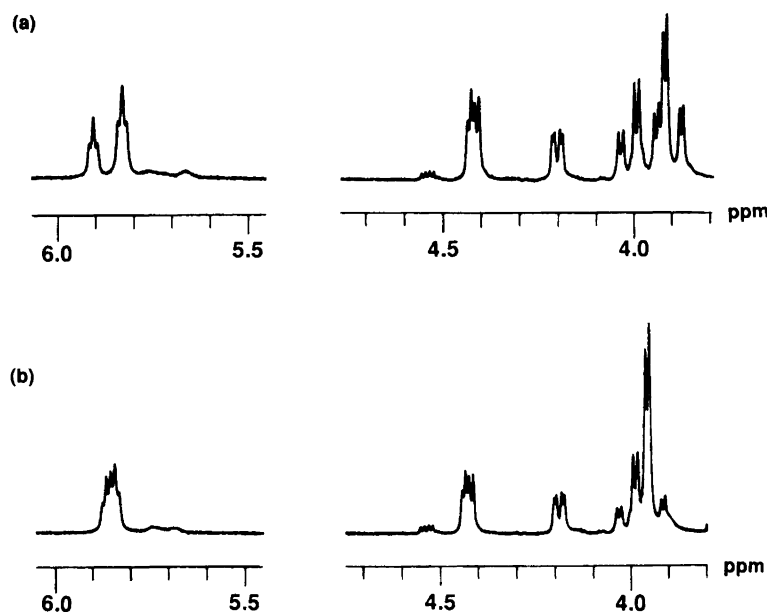


Fig. 1. Partial ¹H NMR spectra of (a) the (R)-1:L-ZGP complex and (b) the (S)-1:L-ZGP complex, showing regions in which the two complexes differ.

Table 2. Counterion structure and enantioselective retention.^a

Solute	Counterion							
	L-ZP		L-ZGP		L-ZGGP		L-CP	
	k'_1	α	k'_1	α	k'_1	α	k'_1	α
1	9.0	1.01	6.4	1.17	9.3	1.14	7.3	1.04
2	0.66	1.00	0.92	1.00	1.0	1.00	0.45	1.00
3	12	1.00	9.7	1.06	13	1.15	6.5	1.00
4	4.9	1.00	4.6	1.05	8.8	1.00	3.7	1.00
5	9.4	1.01	7.1	1.06	8.4	1.35	8.0	1.00
6	—	—	5.1	1.06	8.7	1.07	—	—

^a Solid phase, LiChrosorb DIOL; mobile phase, 2.5 mM of the counterion and 0.20 mM triethylamine in dichloromethane (80 ppm H₂O).

using chiral ion-pair chromatography on different silica phases. Hypercarb is a more homogeneous HPLC-support and consists of hexagonally arranged carbon atoms.¹⁸ Previous studies have shown that porous graphitic carbon is useful as an adsorbing phase for the separation of different types of isomer.¹⁹ The highest separation factor ($\alpha = 2.04$) for the enantiomers of **1** was obtained on this carbon phase, possibly as a result of larger differences in adsorption to the flat Hypercarb surface (K_{RS}^* and K_{SS}^*) of the diastereomeric complexes.

Owing to the large separation factor, complete resolution of the enantiomers of **1** was possible within less than three minutes using Hypercarb as the solid phase [Fig. 4(a)]. The corresponding time for the enantiomeric resolution on LiChrosorb DIOL was about 1 h [Fig. 4(b)].^{6b}

The structure of the solute. Effects of the solute structure on the stereoselective retention using LiChrosorb DIOL

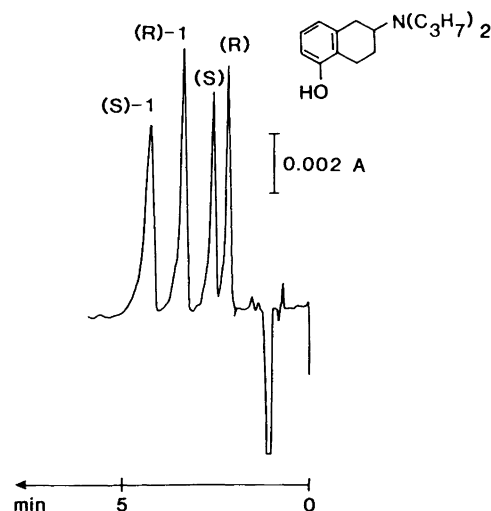


Fig. 2. Enantioselective retention of **1** (left) and the regioisomer 5-hydroxy-2-dipropylaminotetralin (right). Solid phase, Hypercarb; mobile phase, 16 mM L-ZGP in dichloromethane (80 ppm H₂O).

Table 3. Solid phase and stereoselectivity.^a

Solid phase	k'_R	$\alpha_{S/R}$
Polygosil NH ₂	1.4	1.18
Polygosil CN	0.54	1.18
Nucleosil CN	2.6	1.10
Polygosil NO ₂	6.3	1.24
LiChrosorb DIOL	6.4	1.17
Polygosil 7-OH	11	1.12
Hypercarb ^b	3.5	2.04

^a Mobile phase, 2.50 mM L-ZGP and 0.20 mM triethylamine in dichloromethane (80 ppm H₂O); solute, (R,S)-**1**.
^b = 10 mM L-ZGP in dichloromethane (80 ppm H₂O).

Table 4. Solute structure and stereoselectivity on porous graphitic carbon.^a

Solute	k'_1	α
1	3.5	2.04
2	0.57	1.0
3	1.8	1.03
4	0.73	1.16
5	3.7	3.46
6	2.3	1.32

^a Solid phase, Hypercarb; mobile phase, 10 mM L-ZGP in dichloromethane (80 ppm H₂O).

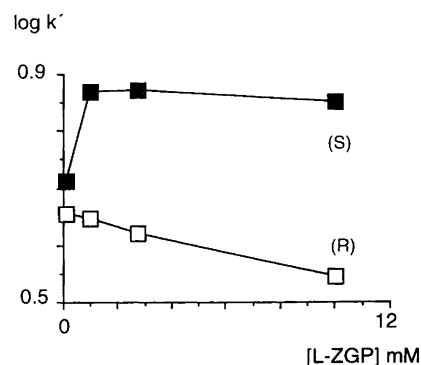


Fig. 3. Influence of chiral counterion concentration on enantioselective retention of **1**. Solid phase, Hypercarb; mobile phase, L-ZGP in dichloromethane (80 ppm H₂O).

Table 5. Solute structure and stereoselectivity on LiChrosorb DIOL.^a

Solute	k'_1	α
1	6.4	1.17
2	0.92	1.0
3	9.7	1.06
4	4.6	1.05
5	7.1	1.06
6	5.1	1.06

^a Solid phase, LiChrosorb DIOL; mobile phase, 2.5 mM L-ZGP and 0.20 mM triethylamine in dichloromethane (80 ppm H₂O).

or Hypercarb as stationary phases are given in Tables 4 and 5. Different mobile phases were used in order to obtain optimum conditions for chiral resolution of the phenolic 2-aminotetralins on the two stationary phases. The retention times were shorter and the separation factors higher using the Hypercarb column. The presence of methyl groups near the stereogenic centre in the 2-aminotetralin influenced the enantioselectivity. By introducing a methyl group in the C2 position (2) the retention time decreased and no chiral discrimination between the enantiomers was obtained. The introduction of a methyl group in the C1 position (3 and 4) decreased

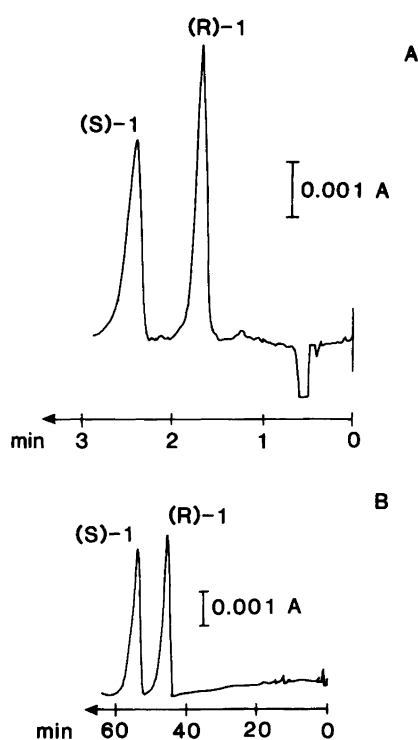


Fig. 4. Solid-phase and enantioselective retention of 1. Chromatographic system A: solid phase, Hypercarb; mobile phase, 10 mM L-ZGP in dichloromethane (80 ppm H₂O); chromatographic system B: solid phase, LiChrosorb DIOL; mobile phase, 2.5 mM L-ZGP and 0.20 mM triethylamine in dichloromethane (80 ppm H₂O).

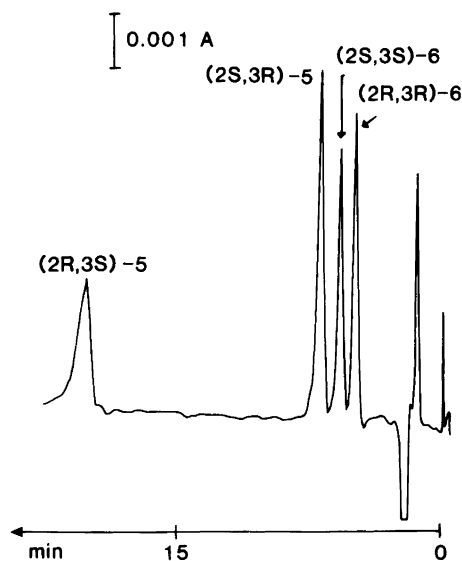


Fig. 5. Separation of stereoisomers of 5 and 6 [from left to right: (2*R*,3*S*)-5, (2*S*,3*R*)-5, (2*S*,3*S*)-6 and (2*R*,3*R*)-6]. Solid phase, Hypercarb; mobile phase, 16 mM L-ZGP in dichloromethane (80 ppm H₂O).

the enantioselectivity when LiChrosorb DIOL or Hypercarb was used as solid phases. On the Hypercarb column the stereoselectivity decreased more for the *cis* isomer (3) and less for the *trans* diastereomer (4). Interestingly, a methyl group in the *cis*-C3-position (5) gave decreased enantioselectivity on the LiChrosorb DIOL column but an increased separation factor was obtained in the Hypercarb system. Finally, introduction of a *trans*-C3 methyl substituent (6) caused a decrease in the separation factor. The separation of the four C3-methyl-substituted stereoisomers (the enantiomers of 5 and 6) are given in Fig. 5.

Theoretical results

A. Conformational properties of the complex components: the phenolic 2-aminotetralin derivatives. It is likely that the enantioselective recognition and binding between molecules is conformationally dependent. In studies of chiral interactions it is, therefore, important to have access to information about the conformational flexibility of the components involved in the recognition process. The conformational preferences of 1–6 have been determined previously²⁰ by use of Allinger's MMP 2 force field²¹ as included in the MIMIC program.²² The results from the calculations are supported by NMR spectroscopy and X-ray crystallography and appear to be reliable.²⁰

When the present investigation was started, parameters for amide and carbamate groups were not included in the MMP2 force field. This prevented us from using MMP2 in calculations involving L-ZGP.²³ Instead we used the MMX force field, which is an extended version of MM2, as included in the PCMODEL program.¹⁰ To investigate how MMX performed compared with

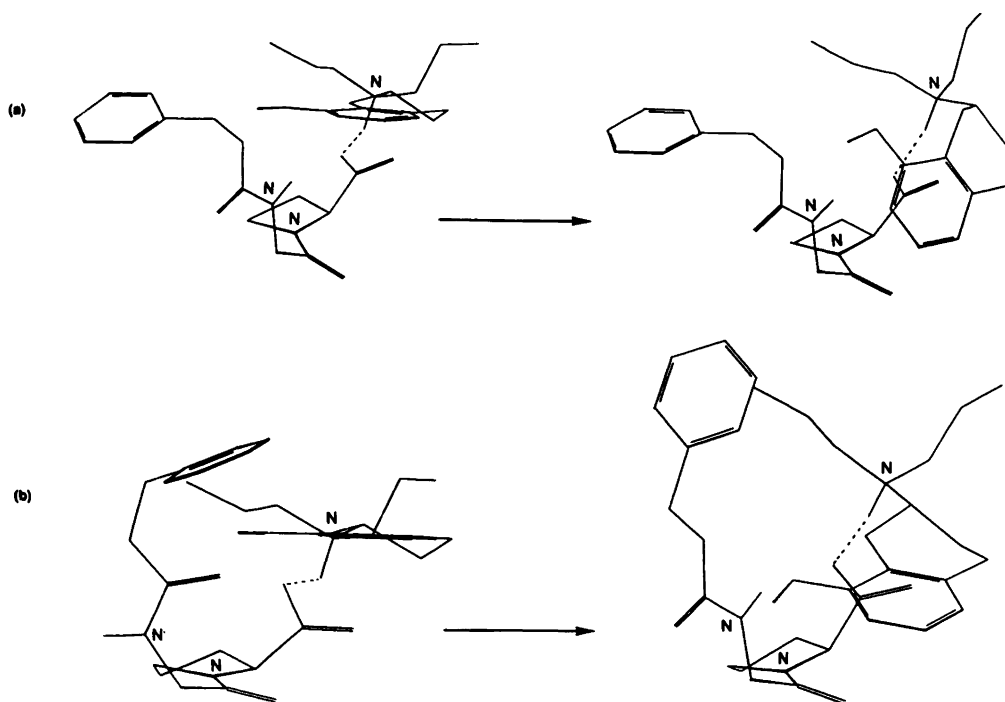


Fig. 6. Geometrical changes during energy minimization: (a) starting geometry (left) and energy-minimized geometry of a complex of (*R*)-**1** and L-ZGP in which the conformation of the non-aromatic ring in **1** changes from a half-chair to a half-boat during the energy minimization; (b) starting geometry (left) and energy-minimized geometry of a complex of (*R*)-**1** and L-ZGP in which the conformation of L-ZGP changes during the energy minimization.

MMP2 in calculations of 2-aminotetralin conformations, we did a complete conformational search on **1**. The results from the MMX and the MMP2 calculations were identical regarding both geometries and relative steric energies, but different absolute values of the steric energies were found. Compound **1** is a fairly flexible molecule with about 40 energetically accessible conformations ($\Delta E_s \leq 3 \text{ kcal mol}^{-1}$).^{*} The methylated compounds **2-6** have different conformational preferences[†] and different steric requirements. However, the primary conformational features of all phenolic 2-aminotetralin derivatives are that they preferentially adopt a half-chair conformation of the non-aromatic ring of the tetralin and a *pseudo*-equatorially oriented dipropylammonium group.²⁰ The agreement between the two force fields indicates that

^{*} The actual number of energetically accessible conformations of **1** is larger than that shown in Ref. 20(a) where only one of the two possible phenolic rotamers was included and the energy cut-off value was $2.5 \text{ kcal mol}^{-1}$.

[†] The conformational properties of **2** are identical with those of the regioisomer, 5-hydroxy-2-methyl-2-dipropylaminotetralin (Johansson, A. M. *Personal communication*). Molecular-mechanics calculations using either the MMP2 or the MMX force field did not reproduce the experimental results of **2**. According to the calculations **2** prefers to adopt a *pseudo*-axial disposition of the dipropylammonium group, however, results from NMR spectroscopy have established that the dipropylammonium substituent is *pseudo*-equatorially oriented. Helander, A. and Kenne, L. *Unpublished results*.

MMX is also an adequate force field in molecular-mechanics calculations of 2-aminotetralins.

L-ZGP. The preferred conformations of L-ZGP in carboxylic acid (neutral) and carboxylate (ionic) forms have been established using the MMX force field.²⁴ The results were compared with NMR data which confirmed the main conformational characteristics.

B. Strategies for the generation of complex geometries. Molecular-mechanics calculations on molecular complexes of the size studied here require a considerable amount of computer time. Consequently, either the number of complex geometries to be examined had to be limited, or the computational effort had to be reduced by other means. In other computational studies of complexes,²⁵ only the global minimum conformations of each complex component were used in the dockings and the atoms in the complexes were fixed during the energy minimizations. The advantage with this strategy is that the time required for calculations is shortened and that a larger number of different complex geometries can be examined (10^5 – 10^6) in a reasonable amount of computer time. However, such a strategy appears less informative when performing calculations on flexible molecules such as those discussed in the present study. It is reasonable to expect that two molecules that approach each other will change conformations to be able to accommodate an optimal fit.^{25m} In addition, available protocols for rigid

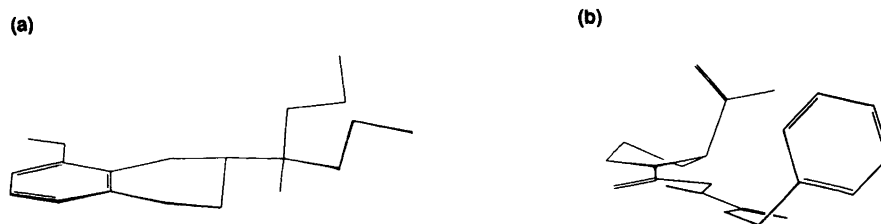


Fig. 7. Conformations of (a) (*R*)-**1** [conformation I in Ref. 20(a)] and (b) L-ZGP (conformation from group 4 in Ref. 24), which were used in the initial studies of intermolecular interactions in the diastereomeric complexes.

dockings produce numerous unproductive dockings in which the two complex components are not aligned to form optimally stable complex structures. Therefore a strategy which uses flexible dockings was assumed to give more realistic results in the present study.

In flexible dockings, all conformations of each complex component are used in the dockings and, to save computer time, the molecules are prealigned to facilitate favourable interactions. Unrestricted energy minimizations are used, that is, all atoms are allowed to move during the energy minimization process. This is important as our results show that both molecules of the complex may change their conformation during the energy minimization/geometry optimization. In some experiments the complex components showed pronounced changes in conformation: for example, the non-aromatic ring of **1** changed from a half-chair to a half-boat conformation during the energy minimization of one complex (Fig. 6).

Manual dockings. In preliminary studies one conformation of (*R*)-**1** and one of L-ZGP were docked manually, using several different alignments, and then energy-minimized. These dockings were performed on a conformation of (*R*)-**1** characterized by $\tau_N = -60^\circ$, $\tau_A = \tau_B = 180^\circ$, $\tau_{A'} = -60^\circ$ and $\tau_{B'} = 180^\circ$ having a relative steric energy (ΔE_s) of $0.6 \text{ kcal mol}^{-1}$.[‡] In this conformation the orientation of the dipropylammonium group of **1** does not prevent a strong ionic interaction with the carboxylate group in L-ZGP. The all-*trans* conformation of L-ZGP was used (Fig. 7). The two complex components were oriented relative to imaginary vectors intersecting the molecules, in L-ZGP along the flat molecule and in **1** from the nitrogen atom across the tetralin moiety (Fig. 8). The vector of **1** was oriented perpendicular to ($+90^\circ$, -90°), in parallel with (0°), and antiparallel (180°) to the L-ZGP vector. As expected, the complexes were stabilized considerably by the reinforced electrostatic interaction and complexes in which the 2-aminotetralin moiety was positioned below or edge-to-face to the L-ZGP molecule were less stable. Complexes were stabilized by intermolecular hydrogen bonding between the carbamate nitrogen and the carboxylate group in L-ZGP, and van der Waals interactions were also important for complex stability; in complexes which were stabilized by

a reinforced ionic interaction, parallel alignment of the molecules resulted in more stable complexes compared with the starting geometries in which the molecular vectors were positioned in a perpendicular or antiparallel manner. In addition, we identified several relative orientations of the two molecules which did not result in stable complex geometries.

The relative orientation of the phenol group was also of importance for complex stability. It has been shown by Karlén *et al.*^{20a} that the phenol group of **1** adopts two in-plane orientations of similar stability, differing only by about $0.1 \text{ kcal mol}^{-1}$ in favour of the conformation with $\tau_{(H-O-C8-C7)} (\tau_{OH}) = 0^\circ$. On rotation of τ_{OH} of the protonated form of **1**, considerably larger energy differences were observed ($1.0 \text{ kcal mol}^{-1}$). Interestingly, when τ_{OH} was driven in one complex of (*R*)-**1** and L-ZGP, the complex with $\tau_{OH} = 180^\circ$ was $1.0 \text{ kcal mol}^{-1}$ more stable than that with $\tau_{OH} = 0^\circ$. In addition, in several of the energy-minimized complexes the phenol group was oriented out of the aromatic plane, indicating that intermolecular interactions may compensate for the destabilization due to an unfavourable geometry around the phenol moiety in protonated **1**.

Multiple minima. The conformational analysis of **1** gave 40 conformations with relative energies below 3 kcal mol^{-1} . For L-ZGP we identified 243 low-energy conformations.²⁴ One would, therefore, have to perform 40×243 different dockings of each enantiomer to take into account the conformational flexibility of the complex components. In fact, the problem is even more complex, since *each conformation of the two species may be oriented*

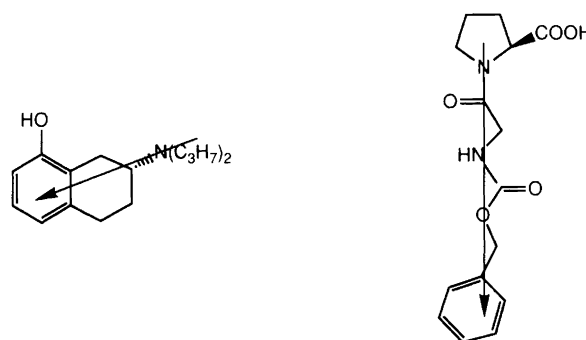


Fig. 8. Description of vectors used in the alignments of the complex components.

[‡] For definitions, see Ref. 20(c). In this initial study conformation I was used.

in an infinite number of ways relative to the other. Therefore, an infinite number of local minima are also to be expected. This was exemplified by an experiment in which starting geometries were generated by changing the angle between the vectors of L-ZGP and (R)-1 in 10° increments from $+90^\circ$ to -90° ; one local minimum was found for each starting geometry (Fig. 9). The multiple local-minima problem has recently been discussed by Scheraga *et al.*²⁶

The manual dockings were performed by aligning the conformation of (R)-1 described above with all possible conformations of L-ZGP generated from the MMX calculations (369 different conformations with relative energies less than $4.6 \text{ kcal mol}^{-1}$) followed by unrestricted energy minimizations. All conformations of L-ZGP identified were used since we believed that even less stable conformations might be stabilized by attractive intermolecular interactions. In the dockings, we attempted to align the molecules to obtain maximum stabilization of the energy-minimized complex. Manual dockings were also made with other conformations of 1, e.g., with a *pseudo-axial* orientation of the dipropylammonium group. However, this resulted in the production of high-energy complex geometries ($\Delta E_s > 4.5 \text{ kcal mol}^{-1}$) or changes in the non-aromatic ring of the tetralin system, thus generating conformations with a *pseudo-equatorially* oriented dipropylammonium group.

Computer-based dockings. Recently, several programs have become available which enable a statistically based conformational search. All rotatable bonds may be moved and the programs generate starting geometries according to certain protocols.²⁷ To check how the results from the manual strategy compares with those from an automatic conformational search we used the BatchMin program included in the MacroModel package to generate complexes between the enantiomers of 1 and L-ZGP.²⁸ The AMBER force field²⁹ was used, since MacroModel does not include the MMX force field, and 10^5 different geometries were searched. In an initial minimization experiment all unique geometries with relative steric energies below 25 kcal mol^{-1} were saved. To limit the computational time, only 10 minimization iterations were allowed. More than 10^4 different geometries of each diastereomeric complex were saved. These geometries were subjected to several subsequent energy minimizations with decreasing energy windows. This process resulted in about 1500 different geometries of each diastereomeric complex with ΔE_s below 5 kcal mol^{-1} .

The three different force fields available in MacroModel, MM2, AMBER and OPLS,³⁰ were used to energy-minimize fully the complex geometries generated. Each force field generated a different set of geometries (about 200 conformations of each diastereomeric complex). To make these complex energies comparable to

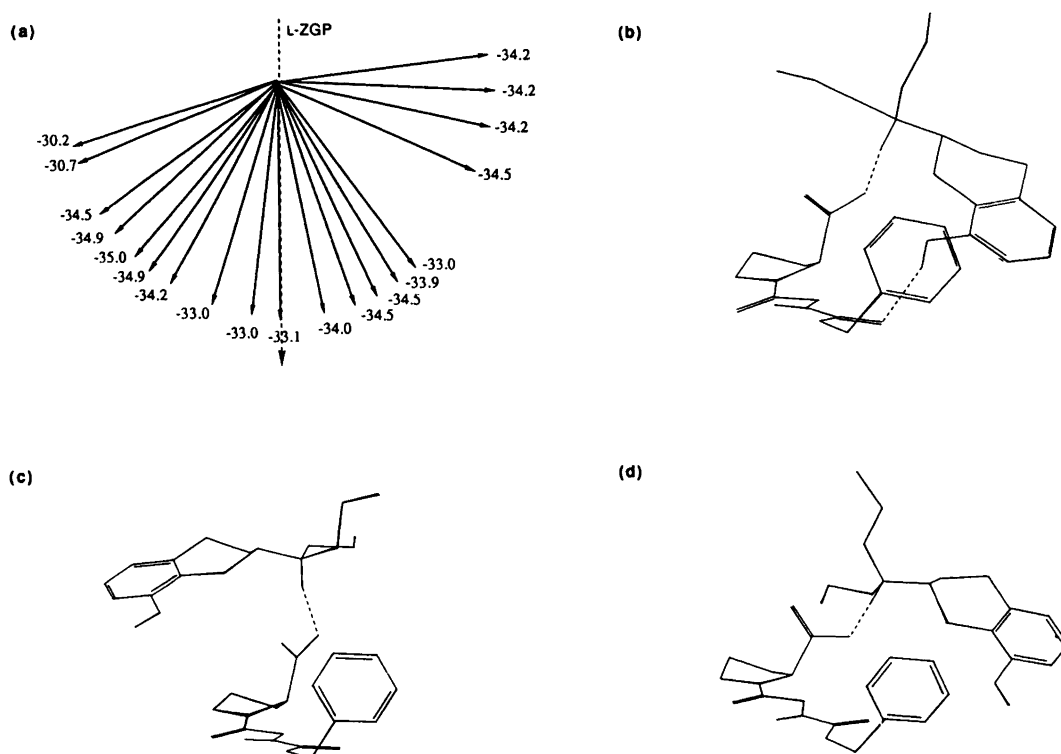


Fig. 9. Multiple complex conformations: (a) MMX energies and vector angles of energy-minimized complexes of (R)-1 and L-ZGP. Starting geometries were varied by changing the vector angle from $+90^\circ$ to -90° in 10° increments. (b) Complex geometry resulting from an aligned vector orientation (0°); (c) and (d) complex geometries resulting from perpendicular vector orientations ($+90^\circ$ and -90° , respectively).

those generated by the manual method, they were finally fully reminimized with the MMX force field.

C. Complex geometries and energies: diastereomeric complexes of L-ZGP and the enantiomers of 1. A total of 750 different complexes of each enantiomer of **1** and L-ZGP were generated by the manual method and then energy minimized. This resulted in the same number of local-minimum conformations, the steric energy range between the most stable and least stable complexes generated from each enantiomer being about 20 kcal mol⁻¹.

The most stable complexes were stabilized by a reinforced electrostatic interaction between the ammonium group in **1** and the carboxylate group of L-ZGP, as well as by other intermolecular hydrogen bonds. In addition, an intramolecular hydrogen bond between the carbamate and carboxylate groups greatly enhances the stability of the complex.

The flexibility of the L-ZGP molecule appears to be considerably restricted in the complexes, since only a limited number of L-ZGP conformations were observed in complex conformers with ΔE_s below 3 kcal mol⁻¹. These L-ZGP conformations showed a predominant *cis*-glycyl-proline amide bond arrangement whereas both *cis* and *trans*-carbamate groups were presented. The conformations of L-ZGP in the (*R*)-**1**: L-ZGP complexes were further characterized by $\psi_{\text{gly}} = +60^\circ$ and $\phi_{\text{gly}} = +60^\circ$ whereas the (*S*)-**1**: L-ZGP complexes showed $\psi_{\text{gly}} = +60^\circ$ and $\phi_{\text{gly}} = 180^\circ$. These L-ZGP conformations allow the formation of the intramolecular hydrogen bond between the carbamate and the carboxylate groups. The benzyl moiety of L-ZGP showed some flexibility since all three *gauche* rotamers were observed in the complexes. Interestingly, the most stable conformation of L-ZGP was not found among complexes with ΔE_s below 4 kcal mol⁻¹.

The random conformational search by BatchMin produced several new complex geometries, some of which showed increased stability compared with those generated manually. The main structural features which distinguish these stable complexes from those found manually, are conformational changes within the dipropylammonium moieties. This result might have been expected since only one conformation of **1** was used in the manual search. This selected conformation was also found among the most stable complexes in the random search, together with one of its τ_N -rotamers ($+60^\circ$). The global minimum conformation of **1** was absent in the most stable complexes produced in the random search, but a similar conformation with $\tau_N = +60^\circ$ was identified. Several high-energy conformations ($\Delta E_s \sim 3$ kcal mol⁻¹) of **1** were found among the most stable complexes. The same set of L-ZGP conformations, observed in stable complexes resulting from the manual search, was also found by the random search.

Diastereomeric complexes of L-ZGP and the enantiomers of 2–6. Manually generated complexes of the enantiomers of **1** and L-ZGP having ΔE_s below 3 kcal mol⁻¹

were used in the construction of starting geometries for complexes of the methylated analogues of **1**. Methyl groups were introduced in the proper positions and the complexes were then subjected to energy minimization.

The same set of L-ZGP conformations were present in energetically stable complexes of **1–6**. It should be noted that the relative orientations of the complex components in complexes containing the methylated derivatives were

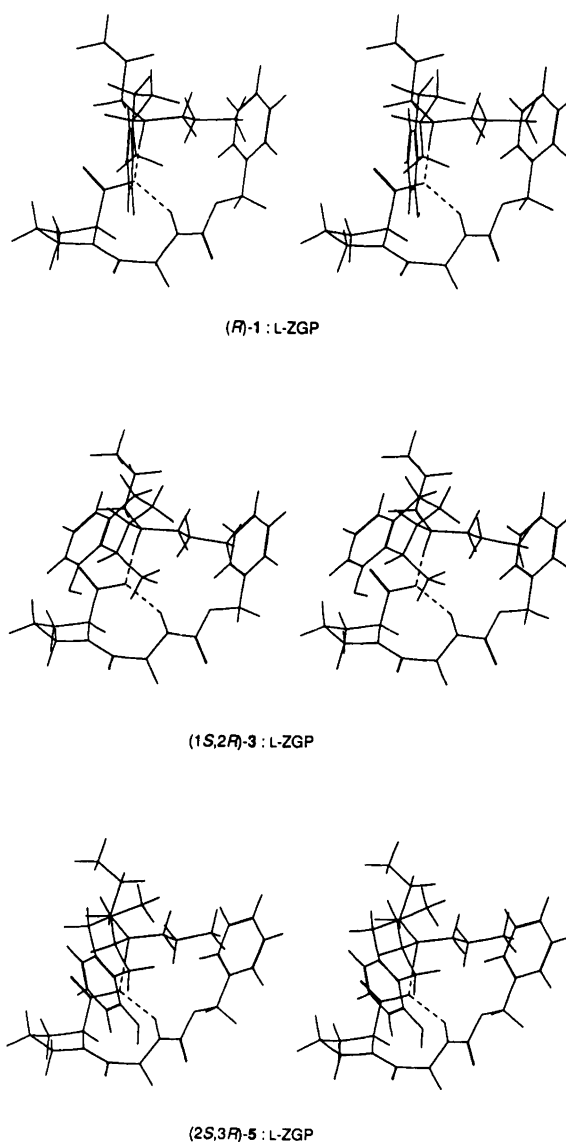


Fig. 10. Stereoscopic representation of changes in complex conformation resulting from the introduction of methyl groups in different positions of the non-aromatic ring of **1**. Energy-minimized complex of (*R*)-**1**: L-ZGP (top); energy-minimized complex resulting from the introduction of a *cis*-1-methyl group forming the (1*S*,2*R*)-**3**: L-ZGP complex (middle); energy minimized complex resulting from introduction of a *cis*-3-methyl group forming the (2*S*,3*R*)-**5**: L-ZGP complex (bottom). Complexes formed by introduction of methyl groups in the *trans* C1 and C3 positions as well as in the C2 position did not show significant changes in the complex geometries compared with (*R*)-**1**: L-ZGP.

Table 6. Dynamic properties^a of energy-minimized (MMX) diastereomeric complexes of **1–6** and L-ZGP. Results are obtained from a combination of data from manual dockings and an automated conformational search.

Complex	MMX-E ^b	Dipole moment ^c	Binding energy ^{b,d}	Surface area/Å ²			
				Total area	Polar area	Unsaturated area	Saturated area
(R)-1: L-ZGP	-41.1	11.7	-46.2	587	95.6	79.4	412.9
(S)-1: L-ZGP	-42.5	14.2	-49.3	588	102.8	77.7	408.8
(R)-2: L-ZGP	-35.6	12.8	-44.2	594	101.1	73.4	417.9
(S)-2: L-ZGP	-36.6	14.6	-44.7	588	106.2	65.2	418.0
(1S,2R)-3: L-ZGP	-36.6	12.6	-44.6	596	98.5	74.5	421.9
(1R,2S)-3: L-ZGP	-36.3	13.3	-44.7	576	93.2	73.6	412.3
(1R,2R)-4: L-ZGP	-37.4	13.3	-43.8	605	102.5	77.7	425.0
(1S,2S)-4: L-ZGP	-37.6	13.5	-42.6	591	99.2	69.4	423.3
(2S,3R)-5: L-ZGP	-39.3	10.5	-41.7	591	95.0	71.8	426.0
(2R,3S)-5: L-ZGP	-38.9	12.4	-42.3	604	95.7	82.9	427.8
(2S,3S)-6: L-ZGP	-37.4	12.9	-45.0	594	97.5	77.8	416.6
(2R,3R)-6: L-ZGP	-39.4	14.2	-47.5	601	103.8	75.8	421.5

^a Calculated according to a Boltzmann distribution at 25°C. ^b kcal mol⁻¹. ^c Debye. ^d Calculated according to Ref. 32.

sometimes different from those of **1**. The differences were largest in the complexes of the 1-methyl and 3-methyl derivatives (**3** or **4** and **5** or **6**, respectively) and smallest in complexes of the 2-methyl analogue (**2**) (Fig. 10).

From a strategical point of view it is interesting to compare the results from the manual strategy with those from the automatic search. Most of the low-energy conformers were generated by the automatic search. However, the manual docking procedure produced most of the low-energy complex geometries of the diastereomeric complexes of **5**. This shows that the two strategies complement each other.³¹

Dynamic complex properties. Results from the MMX calculations are presented in Table 6 which includes the calculated surface areas of the complexes[§] as well as their dipole moments. Also included is the net binding energy for each species. This energy was obtained according to a method described by Boyd *et al.*³² by subtraction of the conformational distortions of the complex components that resulted from the induced fit.

We performed a statistical analysis of potential correlations between the dynamic properties⁴ of the 12 diastereomeric complexes and the chromatographic data, specifically the capacity factor, k' , and the separation

factor, α . Data obtained by the manual method was compared with the total data set. In the data from the manual search there was no correlation between chromatographic results and non-polar surface areas, dipole moments, or steric energies. The only apparent correlation was observed between the separation factor α and the difference in dynamic polar surface area of the diastereomeric complexes, ($r^2 = 0.73$). A better correlation was observed between α and the difference in dynamic unsaturated surface area ($r^2 = 0.80$) when the total data set (a combination of results from the manual and automatic searches) was used.

Concluding remarks

When a chiral counterion is added to the mobile phase, Hypercarb (porous graphitic carbon, PGC) with its flat adsorbing surface displays efficient enantioselective discrimination between the enantiomers of **1–6**, resulting in baseline separation of several of the solutes. The stereoselectivity is dependent on the structure of both the counterion and the solutes. The differences in retention and stereoselectivity for **2–6** may be explained by the added methyl group which influences the conformation of the diastereomeric complexes and therefore also the adsorption to the stationary phase. The steric bulk of the methyl group protruding from the surface of the complex, may result in a decrease of the adsorption.³³ This phenomenon is mainly observed in complexes of **2** for which k' has the lowest value (0.56) and $\alpha = 1.0$.

The highest separation factors (α) are obtained at a high counterion concentration, which indicates that the enantioselectivity is based mainly on differences in the degree of adsorption of the diastereomeric complexes

[§] Surface areas were calculated using a grid size of 0.1 Å. The total surface was divided into polar and non-polar surface areas and the non-polar surface was further divided into saturated and unsaturated non-polar surface areas. Since the complexes are formed from flexible molecules the data were statistically averaged according to a calculated Boltzmann distribution (25°C) to give the dynamic properties of each set of complexes (cf. Ref. 4).

to the PGC surface. Also, the results obtained from molecular-mechanics calculations indicate that the chromatographic separation of the enantiomers of the six 2-aminotetralin derivatives is determined by the difference in adsorption of the diastereomeric complexes to the stationary phase. Since the differences in dynamic unsaturated surface area of the complexes correlate reasonably well with the separation factors, the separation process may be determined by the strength of the interactions between aromatic systems.

Acknowledgments. Financial support was provided by the Swedish Natural Science Research Council and the Swedish National Board for Industrial and Technical Development. We also thank Professor Kosta Steliou for providing a copy of the PCMODEL program.

References

- Resolution of amino acids and amines following derivatization with *N*-TFA-prolyl chloride: Karger, B. L., Stern, R. L. and Keane, W. *Anal. Chem.* 39 (1967) 228; Resolution of hydroxy acids and alcohols following derivatization with 2-phenylpropionyl chloride: Hammarström, S. and Hamberg, M. *Anal. Biochem.* 52 (1973) 169; Resolution of carboxylic acids following derivatization with 1-(1-naphthyl)ethylamine: Vecchi, M. and Müller, R. K. *J. High Resol. Chromatogr. Chromatogr. Commun.* (1983) 612; Resolution of amino alcohols following derivatization with *N*-TFA-prolyl chloride: Silber, B. and Riegelman S. *J. Pharm. Exp. Ther.* 221 (1980) 109.
- See, for example: (a) Armstrong, D. W., Alak, A., DeMond, W., Hinze, W. L. and Riehl, T. E. *J. Liq. Chromatogr.* 8 (1985) 261; (b) Allenmark, S., Bomgren, B. and Boren, H. *J. Chromatogr.* 252 (1982) 297; (c) Hermansson, J. and Eriksson, M. *J. Liq. Chromatogr.* 9 (1986) 621; (d) Pirkle, W. H. and Pochapsky, T. C. *Chem. Rev.* 89 (1989) 347; (e) Erlandsson, P., Marle, I., Hansson, L., Isaksson, R., Pettersson, C. and Pettersson, G. *J. Am. Chem. Soc.* 112 (1990) 4573.
- See, for example: (a) Pirkle, W. H. and House, D. W. *J. Org. Chem.* 44 (1979) 1957; (b) Hare, P. E. and Gil-Av, E. *Science* 104 (1979) 1226; (c) Pettersson, C. and Schill, G. *J. Chromatogr.* 204 (1981) 179; (d) Debowski, J., Sybilska, D. and Jurczak, J. *Chromatographia* 16 (1982) 198.
- Lipkowitz, K. B., Baker, B. and Larter, R. *J. Am. Chem. Soc.* 111 (1989) 7750.
- Thomson, A. and Kapadia, S. B. *Eur. J. Biochem.* 102 (1979) 117.
- Synthesis and resolution of **1**: (a) Arvidsson, L.-E., Hacksell, U., Nilsson, J. L. G., Hjort, S., Carlsson, A., Lindberg, P., Sanchez, D. and Wikström, H. *J. Med. Chem.* 24 (1981) 921; (b) Karlsson, A., Pettersson, C., Sundell, S., Arvidsson, L.-E. and Hacksell, U. *Acta Chem. Scand., Ser. B* 42 (1988) 231; (c) Arvidsson, L.-E., Hacksell, U., Johansson, A. M., Nilsson, J. L. G., Lindberg, P., Sanchez, D., Wikström, H., Svensson, K., Hjort, S. and Carlsson, A. *J. Med. Chem.* 27 (1984) 45.
- Synthesis of **2**: Mellin, C., Liu, Y., Hacksell, U., Björk, L. and Andén, N.-E. *Acta Pharm. Suec.* 24 (1987) 153.
- Synthesis of **3** and **4** and resolution of **3**: Arvidsson, L.-E., Johansson, A. M., Hacksell, U., Nilsson, J. L. G., Svensson, K., Hjorth, S., Magnusson, T., Carlsson, A., Andersson, B. and Wikström, H. *J. Med. Chem.* 30 (1987) 2105.
- Synthesis and resolution of **5** and **6**: Mellin, C., Björk, L., Karlén, A., Johansson, A. M., Sundell, S., Kenne, L., Nelson, D. L., Andén, N.-E. and Hacksell, U. *J. Med. Chem.* 31 (1988) 1130.
- Gajewski, J. J., Gilbert, K. E. and McKelvey, J. *Adv. Mol. Model.* 2 (1990) 65. The PCMODEL program is available from Serena Software, Bloomington, IN, 47402-3076 USA. The program has been reviewed by Freeman, P. K. *J. Am. Chem. Soc.* 111 (1989) 1942.
- Snyder, L. R. and Kirkland, J. J. *Introduction to Modern Liquid Chromatography*, Wiley-Interscience, New York 1979.
- Karlsson, A. and Pettersson, C. *J. Chromatogr.* 543 (1991) 287.
- Karlsson, A., Huyhn, N. H. and Pettersson, C. *In preparation*.
- Karlsson, A. and Pettersson, C. *Chirality.* 9 (1992) 323.
- Pearson, R. G. and Vogelsson, D. C. *J. Am. Chem. Soc.* 80 (1957) 1038.
- Pettersson, C. *J. Chromatogr.* 316 (1984) 553.
- Pettersson, C., Karlsson, A. and Gioeli, C. *J. Chromatogr.* 407 (1987) 217.
- Knox, J. H. and Kaur, B. In: Brown P. R. and, Hartwick, R. A., Eds., *High Performance Liquid Chromatography*, Wiley, New York 1989, 189.
- Gilbert, M. T., Knox, J. H. and Kaur, B. *Chromatographia* 16 (1982) 138.
- (a) Conformational analysis of **1**, **3** and **4**: Arvidsson, L.-E., Karlén, A., Norinder, U., Kenne, L., Sundell, S. and Hacksell, U. *J. Med. Chem.* 31 (1988) 212; (b) Conformational analysis of **5** and **6**: *Ref. 9(c)*; (c) the conformational space of the 5-hydroxy isomer of **2** has been investigated: Karlén, A., Johansson, A. M., Kenne, L., Arvidsson, L.-E. and Hacksell, U. *J. Med. Chem.* 29 (1986) 917.
- Allinger, N. L. *J. Am. Chem. Soc.* 99 (1977) 8127.
- Liljefors, T. *Mol. Graphics* 1 (1983) 11.
- Parameters for the amide functionality are included in the latest version of MMP2. However, parameters for the carbamate group are still absent. For MM2 calculations of amides, see (a) Lii, J.-H., Gallion, S., Bender, C., Wikström, H., Allinger, N. A., Flurchick, K. M. and Teeter, M. M. *J. Comput. Chem.* 10 (1989) 503; (b) Schnur, D. M., Yuh, Y. H. and Dalton, D. R. *J. Org. Chem.* 54 (1989) 3779.
- Luthman, K. and Hacksell, U. *Acta Chem. Scand.* 47 (1993) 461.
- (a) Lipkowitz, K., Landwer, J. M. and Darden, T. *Anal. Chem.* 58 (1986) 1611; (b) Lipkowitz, K. B., Malik, D. J. and Darden, T. *Tetrahedron Lett.* 27 (1986) 1759; (c) Lipkowitz, K. B., Demeter, D. A., Parish, C. A. and Darden, T. *Anal. Chem.* 59 (1987) 1731; (d) Lipkowitz, K. B., Demeter, D. A., Parish, C. A., Landwer, J. M. and Darden, T. *J. Comput. Chem.* 8 (1987) 753; (e) Norinder, U. and Sundholm, E. G. *J. Liq. Chromatogr.* 10 (1987) 2825; (f) Topiol, S., Sabio, M., Moroz, J. and Caldwell, W. B. *J. Am. Chem. Soc.* 110 (1988) 8367; (g) Lipkowitz, K. B., Demeter, D. A., Zegarra, R., Larter, R. and Darden, T. *J. Am. Chem. Soc.* 110 (1988) 3446; (h) Topiol, S. and Sabio, M. *J. Chromatogr.* 461 (1989) 129; (i) Lipkowitz, K. B., Baker, B. and Zegarra, R. *J. Comput. Chem.* 10 (1989) 718; (j) Lipkowitz, K. B., Baker, B. and Larter, R. *J. Am. Chem. Soc.* 111 (1989) 7750; (k) Lipkowitz, K. B., Antell, S. and Baker, B. *J. Org. Chem.* 54 (1989) 5449; (l) Still, M. G. and Rogers, L. B. *Talanta* 36 (1989) 35; (m) Still, M. G. and Rogers, L. B. *J. Comput. Chem.* 11 (1990) 242; (n) Lipkowitz, K. B. and Baker, B. *Anal. Chem.* 62 (1990) 774.
- Ripoll, D. R. and Scheraga, H. A. *Biopolymers* 30 (1990) 165.
- (a) Ferguson, D. M. and Raber, D. J. *J. Am. Chem. Soc.* 111 (1989) 4371; (b) Saunders, M., Houk, K. N., Wu, Y.-D., Still, W. C., Lipton, M., Chang, G. and Guida, W. C. *J. Am. Chem. Soc.* 112 (1990) 1419; (c) Saunders, M. and Krause, N. *J. Am. Chem. Soc.* 112 (1990) 1791; (d) Froimowitz, M. *Biopolymers* 30 (1990) 1011.

28. Mohamadi, F., Richards, N. G. J., Guida, W. C., Liskamp, R., Lipton, M., Caufield, C., Chang, G., Hendrickson, T. and Still, W. C. *J. Comput. Chem.* 11 (1990) 440.
29. (a) Weiner, S. J., Kollman, P. A., Case, D. A., Singh, U. C., Ghio, C., Alagona, G., Profeta, S. and Weiner, P. *J. Am. Chem. Soc.* 106 (1984) 765; (b) Weiner, S. J., Kollman, P. A., Nguyen, D. T. and Case, D. A. *J. Comput. Chem.* 7 (1986) 230.
30. Tirado-Rives, J. and Jorgensen, W. *J. Am. Chem. Soc.* 110 (1988) 1657.
31. Däppen, R., Karfunkel, H. R. and Leusen, F. J. J. *J. Comput. Chem.* 11 (1989) 181.
32. Boyd, F. L., Cheatham, S. F., Remers, W., Hill, G. C. and Hurley, L. H. *J. Am. Chem. Soc.* 112 (1990) 3279.
33. Kiselev, A. V. and Yashin, Y. I. *Gas Adsorption Chromatography*, Plenum Press, New York 1969.

Received June 12, 1992.